MOLECULAR AND CELLULAR BIOLOGY, Aug. 2000, p. 5690–5699 Vol. 20, No. 15
0270-7306/00/$04.00+0

Evidence for a Telomere-Independent "Clock" Limiting *RAS* Oncogene-Driven Proliferation of Human Thyroid Epithelial Cells

C. J. JONES,[1] D. KIPLING,[1] M. MORRIS,[1] P. HEPBURN,[1] J. SKINNER,[1] A. BOUNACER,[1] F. S. WYLLIE,[1] M. IVAN,[1] J. BARTEK,[2] D. WYNFORD-THOMAS,[1]* AND J. A. BOND[1]

Cancer Research Campaign Laboratories, Department of Pathology, University of Wales College of Medicine, Heath Park, Cardiff CF14 4XN, United Kingdom,[1] and Institute of Cancer Biology, Danish Cancer Society, DK-2100 Copenhagen, Denmark[2]

Received 9 December 1999/Returned for modification 3 January 2000/Accepted 27 April 2000

An initiating role for *RAS* oncogene mutation in several epithelial cancers is supported by its high incidence in early-stage tumors and its ability to induce proliferation in the corresponding normal cells in vitro. Using retroviral transduction of thyroid epithelial cells as a model we ask here: (i) how mutant RAS can induce long-term proliferation in an epithelial cell in contrast to the premature senescence observed in fibroblasts; and (ii) what is the "clock" which eventually triggers spontaneous growth arrest even in epithelial clones generated by mutant RAS. The early response to *RAS* activation in thyroid epithelial cells showed two features not seen in fibroblasts: (i) a marked decrease in expression of the cyclin-dependent kinase inhibitor (CDKI) $p27^{kip1}$ and (ii) the absence of any induction of $p21^{waf1}$. When proliferation eventually ceased (after up to 20 population doublings) this occurred despite undiminished expression of mutant RAS and was tightly correlated with a return to the initial high level of $p27^{kip1}$ expression, together with the de novo appearance of $p16^{ink4a}$. Importantly, neither the CDKI changes nor the proliferative life span of RAS-induced epithelial clones was altered by induction of telomerase activity through forced expression of the catalytic subunit, hTERT, at levels sufficient to immortalize human fibroblasts. These data provide a basis for cell-type differences in sensitivity to RAS-induced proliferation which may explain the corresponding tumor-type specificity of RAS mutation. They also show for the first time in a primary human cell model that a telomere-independent mechanism can limit not only physiological but also oncogene-driven proliferation, pointing therefore to a tumour suppressor mechanism additional, or alternative, to the telomere clock.

RAS mutation occurs at high frequency in several human epithelial tumor types, notably those of colon (8), pancreas (1), and thyroid (36, 58). Analyses of clinical samples indicate its involvement at early (premalignant) stages and in pancreas and thyroid are consistent with a role as the initiating molecular event. In the case of thyroid, where a suitable cell culture model exists, this has been strongly supported by the results of in vitro gene transfer experiments (7, 37). Whereas normal thyrocytes exhibit a very low proliferative rate (as is also the case in the intact gland) and cease growing in even optimal culture conditions after less than 3 population doublings (PD), introduction of mutant RAS induces a dramatic proliferative response, resulting in generation of clones whose final size (up to 10^7 cells) and well-differentiated phenotype are consistent with those of a small benign thyroid tumor (adenoma) in vivo (7).

This prolonged clonal expansion contrasts sharply with the more widely studied effects of *RAS* mutation in primary fibroblasts (39, 55, 73), in which proliferation is sharply limited by induction of a premature senescence state. Nevertheless, even in thyrocytes, proliferation does not continue indefinitely and eventually spontaneously ceases after 15 to 25 PD (7, 37), terminating in a viable state of growth arrest, resembling replicative senescence. Spontaneous immortalization has never been observed despite many hundreds of gene transfer experiments in our laboratory.

In vivo, the vast majority of thyroid adenomas also appear to reach a self-limiting quiescent end point. Such limitations in tumor growth are often ascribed to insufficient ability to promote new blood vessel formation and/or to invade surrounding tissues. Importantly, however, the observation that a restriction similar to clonal expansion occurs even in tissue culture indicates, on the contrary, that a cell-intrinsic mechanism which is independent of tissue architecture and is most likely to be based on number of elapsed cell divisions is responsible.

Interest in intrinsic proliferative life span barriers (PLBs) (4, 52, 69) has been heightened recently by the demonstration that one such cell division "clock" is based on the progressive shortening of chromosome telomeres, which has been shown to trigger replicative senescence in a number of normal human cell types (3) by a pathway involving p53 (5, 21) and the cyclin-dependent kinase inhibitor (CDKI) $p21^{Waf1}$ (11). Here we have set out to examine the relationship between this mechanism and that responsible for limiting the proliferative response to activated RAS in thyroid epithelial cells. In striking contrast to the fibroblast paradigm, the results point to a telomere-independent clock operating through a distinctly different set of CDKI changes, which may represent a novel class of PLB responsible for arresting oncogene-induced tumor development in some types of human epithelial cells at an early (premalignant) stage.

* Corresponding author. Mailing address: Cancer Research Campaign Laboratories, Department of Pathology, University of Wales College of Medicine, Heath Park, Cardiff CF14 4XN, United Kingdom. Phone: 44 (029) 2074 2700. Fax: 44 (029) 2074 2704. E-mail: KingTD@Cardiff.ac.uk.

MATERIALS AND METHODS

Cells and culture conditions. Primary monolayer cultures of follicular epithelial cells (>99% epithelial as judged by cytokeratin immunostaining) were prepared from surgical samples of normal thyroid tissue by protease digestion and mechanical disaggregation (66) and maintained in a 2:1:1 mixture of Dulbecco's modified Eagle's medium, Ham's F-12 medium, and MCDB104 (all from Life Technologies, Paisley, United Kingdom) (7) supplemented with 10% fetal calf serum (Imperial Laboratories, London, United Kingdom). Normal human diploid fibroblasts (HCA2 cells, kindly provided by James Smith, Houston, Texas) were grown in Dulbecco's modified Eagle's medium (Life Technologies) supplemented with 10% fetal calf serum (Imperial Laboratories). Senescence occurred at an estimated PD level of 65 to 70.

Retroviral vectors. Replication-defective amphotropic retroviral vectors encoding the Val-12 mutant of human H-RAS (psi-CRIP-DOEJ) together with the *neo* gene for selection in G418 and the vector-only control (psi-CRIP-neo) were used as previously described (7). To allow dual selection, we constructed retrovirus vectors for hTERT and HPV E7 based on pBABEpuro (46), which confers resistance to puromycin. pBABEpuro-hTERT has been described recently (68); pBABEpuro-E7 was constructed by PCR synthesis of the E7 open reading frame together with a consensus upstream Kozak sequence and appropriate restriction sites to allow ligation into the *Bam*HI and *Eco*RI sites of pBABEpuro.

Retroviral gene transfer. Primary thyroid epithelial cells were plated at $\sim 5 \times 10^5$ per 60-mm-diameter dish and infected 2 days later with retrovirus-containing medium from near-confluent producer cells, containing 8 μg of Polybrene per ml (7). Three days later, cells were passaged and maintained in medium with or without G418 (400 μg/ml) or puromycin (2.5 μg/ml) as indicated.

Assessment of DNA synthesis by BrdU incorporation. Cells were labeled by incubation in 10 μM bromodeoxyuridine (BrdU) for 1 h, following which nuclear incorporation was detected by immunoperoxidase immunocytochemistry as previously described (4). The proportion of labeled nuclei (labeling index [LI]) was determined from a count of >500 cells per datum point.

Analysis of mutant RAS expression by reverse transcription-PCR. Poly(A)$^+$ RNA was extracted from normal monolayers or from pooled colonies generated by retroviral vector DOEJ, using a Micro-FastTrack mRNA isolation kit (Invitrogen Corp., San Diego, Calif.). A partial H-ras cDNA was synthesized using a reverse transcription-PCR kit (Perkin-Elmer Cetus, Norwalk, Conn.) with primer 5′-TGGACGAATACGACCCCACT-3′, located downstream of codon 12. This was then amplified using this primer together with upstream primer 5′-CTGAGGAGCGATGACGGAAT-3′ in a PCR mixture consisting of 30 cycles of 1-min denaturation at 94°C, 1-min annealing at 60°C, and 1-min extension at 72°C, with an additional 4-min extension after the final cycle. A single 95-bp product was seen on gel electrophoresis. This was then sequenced using an ABI-Prism cycle sequencing kit (PE-Applied Biosystems) with the downstream primer described above.

Detection of SAβ-Gal activity. Endogenous senescence-associated mammalian β-galactosidase activity (SAβ-Gal) (15) was assessed histochemically (7) using X-Gal substrate (5-bromo-4-chloro-3-indolyl-β-D-galactopyranoside).

Immunocytochemical analysis. For $p16^{ink4a}$, monolayers were fixed in acetone-methanol, 1:1 (10 min at −20°C), and a standard indirect immunoperoxidase procedure applied, using mouse monoclonal antibody DCS-50 (43) (Oncogene Research Products), followed by peroxidase-conjugated rabbit anti-mouse immunoglobulin (Ig) (Dako). A similar procedure was followed for H-RAS using monoclonal Y13-259 followed by swine-anti-rat Ig-peroxidase (Dako) and for the corresponding rat control antibody (antipolyoma large T).

For $p21^{waf1}$, $p27^{kip1}$, and cyclin D1, cultures were fixed in 4% paraformaldehyde (10 min; or 4 min in the case of cyclin D1) and then pretreated with 50 mM glycine (10 min), 0.2% Triton X-100 (10 min), and 0.3% H_2O_2 (3 min), and nonspecific binding was blocked with 2% horse serum (30 min). Anti-p21 (Clone 6B6; Cambridge Bioscience, Cambridge, United Kingdom), anti-p27 (Transduction Laboratories), or anti-cyclin D1 (DCS-6; Santa Cruz) mouse monoclonal antibodies were applied followed by the mouse-specific avidin-biotin-peroxidase (ABC) system (Novocastra).

For cyclin D3, cells were fixed in 2% paraformaldehyde and then permeabilized in methanol followed by 0.1% Triton X-100 as described (14). Detection was by the ABC method using monoclonal antibody DCS-22 clone E8 (2) as the primary antibody.

For all antigens, sites of antibody binding were visualized by the deposition of brown polymer following incubation in diaminobenzidine-hydrogen peroxide solution.

Immunoblotting. Cells were lysed for 5 min at 4°C by 1% NP-40 in 150 mM NaCl, 50 mM Tris (pH 8.0), and 5 mM EDTA buffer, which contained 1 mM phenylmethylsulfonyl fluoride and 0.01 mg each of aprotinin and leupeptin per ml. Protein samples (30 μg) were separated by sodium dodecyl sulfate–12% polyacrylamide gel electrophoresis and electroblotted to Transblot polyvinylidene difluoride membrane (Bio-Rad Labs, Hemel Hempstead, United Kingdom). Anti-p16 antibody (as above) was applied, followed by goat anti-mouse Ig-peroxidase conjugate and visualization by the ECL detection system (Amersham, Little Chalfont, United Kingdom). The filter was stained with India ink, and quantitation of the specific signal and the amount of protein loaded was performed using a Bio-Rad imaging densitometer running Molecular Analyst software.

TRF length analysis. Genomic DNA (1 μg), prepared as previously described (30), was digested with 10 U each of *Rsa*I and *Hin*fI and separated on 0.5% agarose Tris-borate-EDTA gels. Gels were denatured with 1.5 M NaCl–0.5 M NaOH (15 min), neutralized with 1.5 M NaCl–0.5 M Tris, pH 8.0 (10 min), and then dried onto 3MM paper (Whatman) for 1 h at room temperature followed by 30 min at 60°C. Gels were then removed from the paper and hybridized at 37°C overnight in 5× SSC (1× SSC is 0.15 M NaCl plus 0.015 M sodium citrate)–5× Denhardt's–0.5 mM pyrophosphate–10 mM Na_2HPO_4 with a single-stranded DNA probe $(CCCTAA)_3$ (500 ng/gel), which was end-labeled with [γ-^{32}P]ATP (3,000 Ci/mmol) by 10 U of T4 polynucleotide kinase (Amersham). After washing with three changes of 0.1× SSC at 37°C and two at room temperature, gels were wrapped in Saran and signals were detected using a STORM phosphorimager (Amersham Pharmacia Biotech) from which mean terminal restriction fragment (TRF) length was calculated (35) using Molecular Analyst software (Bio-Rad).

Telomere repeat amplification protocol (TRAP assay). Cells (10^7 per 185 μl) were lysed in hypotonic-detergent buffer (1 mM Tris-HCl [pH 7.5], 1 mM $MgCl_2$, 1 mM EGTA, 1 mM phenylmethylsulfonyl fluoride, 5 mM 2-mercaptoethanol, 0.5% 3-[(3-cholamidopropyl)-dimethylammonio]-1-propanesulfonate (CHAPS), 10% glycerol) for 30 min on ice followed by centrifugation at 100,000 × *g* for 30 min at 4°C. Extracts (3,000 cell equivalents) were assayed with or without pretreatment for 10 min at 85°C (to abolish telomerase activity).

Telomerase activity was assayed according to the standard TRAP protocol (32) except that the wax barrier was avoided and *Taq* polymerase and the second primer, CX, were added to reaction mixtures prewarmed to 92°C following elongation of the TS primer. Telomerase products were resolved in 10% polyacrylamide gels and visualized by Sybr Gold staining and fluoroimaging, again using a STORM system. Extracts of cell line 293 were used as a positive control (10). The incorporation of an internal standard (67) demonstrated that there were no inhibitors of PCR detectable with the quantities of protein used.

RESULTS

Induction of thyrocyte proliferation by mutant RAS correlates with reduced nuclear $p27^{kip1}$ expression. Normal human thyroid epithelial cells in primary culture were stably transduced with an amphotropic retroviral vector encoding mutant (V12) H-RAS. As described previously (7), this results in the generation of rapidly growing colonies (approximately 50 per dish of 10^5 cells infected) which are clearly distinguishable from the surrounding uninfected monolayer by 7 to 10 days after infection. Normal (uninfected) thyroid cells cease proliferating after <3 PD and, even prior to this, exhibit a very low proliferative rate, which accounts for the low yield of transduced cells compared to that seen for example with fibroblast cell lines.

Using immunocytochemistry to permit analysis of small cell numbers and to reveal changes in subcellular distribution, we initially examined the expression of several cell cycle regulators which have been implicated in RAS-induced proliferation in other models, namely cyclin D1, $p21^{waf1}$, and $p27^{kip1}$. We also included cyclin D3, which has been shown to play a particularly important role in normal thyroid epithelial cells (14).

Normal thyrocytes, after 7 days in culture, expressed readily detectable levels of cyclin D1, D3, (not shown), and p21 in the majority of nuclei (Fig. 1a); in particular nearly 100% of cells exhibited strong nuclear immunostaining for p27 (Fig. 1a). As expected, the BrdU LI was extremely low (<1%) and nearly all cells were positive for SAβ-Gal, which has been widely reported as a marker of replicative senescence in other cell types (15).

In colonies induced to proliferate by mutant RAS at the earliest time point analyzable (7 to 10 days) BrdU LI had increased to 36%, accompanied by a fall in the SAβ-Gal index to 7%. This proliferative response was associated with a slight reduction in the proportion of cells expressing detectable nuclear p21, which failed to reach statistical significance, and an increase in the proportion expressing cyclin D1 from ~70% to nearly 100% (Fig. 1a and c). Cyclin D3 expression remained essentially unchanged at this (and subsequent) time point at between 50 and 60% of nuclei (not shown). The major change observed however was a marked fall in p27 expression, which

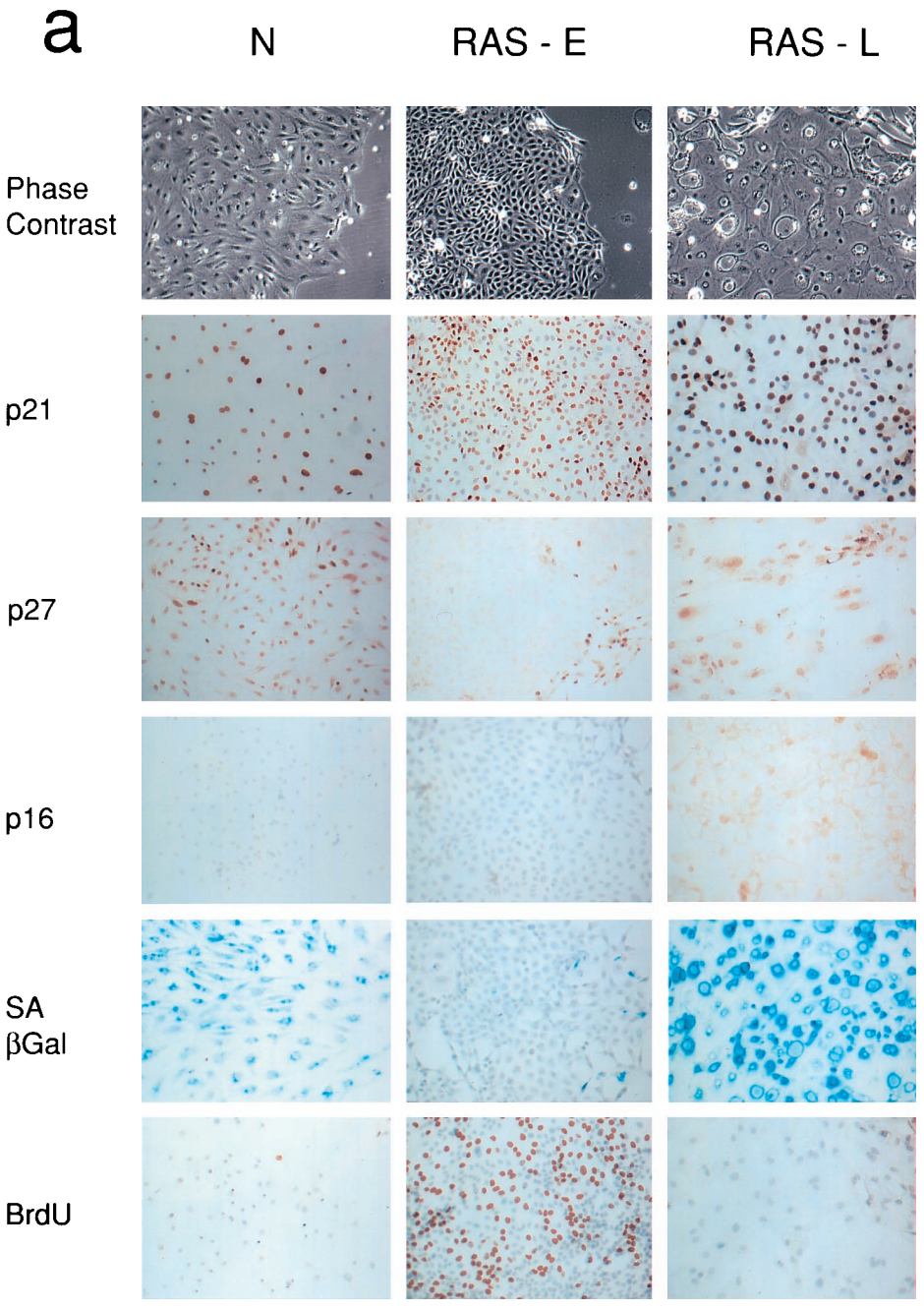

FIG. 1. Expression of cell cycle regulators during the life span of thyroid epithelial clones induced to proliferate by mutant RAS. (a) Representative photomicrographs of normal thyroid epithelial cells (N) and colonies induced by mutant RAS at an early rapidly proliferating stage (RAS-E) and at a late stage at the end of their proliferative life span (RAS-L). Expression of $p21^{waf1}$, $p27^{kip1}$, and $p16^{ink4a}$ and incorporation of BrdU were analyzed by immunocytochemistry (positivity indicated by brown peroxidase reaction product); the senescence-associated marker SAβ-Gal was assessed by X-Gal histochemistry (blue reaction product). In some panels, nuclei are lightly counterstained with hematoxylin to aid visualization. Note a reduction in nuclear p27 correlating with high BrdU labeling in RAS-E colonies and the increase in p16 in RAS-L colonies (magnification ×25). (b and c) Quantitative analyses of normal epithelial cells and colonies expressing mutant RAS at early (1 to 2 weeks), middle (2 to 3 weeks), and late (>5 weeks) stages showing an inverse correlation between a proportion of nuclei containing detectable p27 (■) and a proportion in cell cycle S phase as shown by BrdU incorporation (●) and a direct correlation between p27 and SAβ-Gal expression (▲) note less-marked changes in proportions of nuclei containing detectable p21 (□) and cyclin D1 (○). Results are presented as means of >300 cells per datum point ± standard errors of the mean (error bars). (d) Western blot-ECL analysis of $p16^{ink4a}$ expression (upper panel) in normal thyroid epithelial cells (N), RAS-induced colonies at an intermediate stage of their life span (RAS MID), and end-stage colonies (RAS L). The lower panel shows part of an India ink-stained filter to assess equality of protein loading. Figures show integrated optical density values obtained by scanning densitometry from which the relative increase in p16 signal corrected for total protein between RAS MID and RAS L is calculated at 20-fold.

was detectable in only 16% of cells (nuclei) expressing mutant RAS, compared to 95% in the surrounding normal monolayer (Fig. 1a and b).

To control for the possibility that the reduction in p27 content in early RAS-induced colonies might merely be a secondary consequence of the much higher proportion of proliferating cells, we also examined an analogous model in which primary thyrocytes are induced to proliferate by simian virus 40

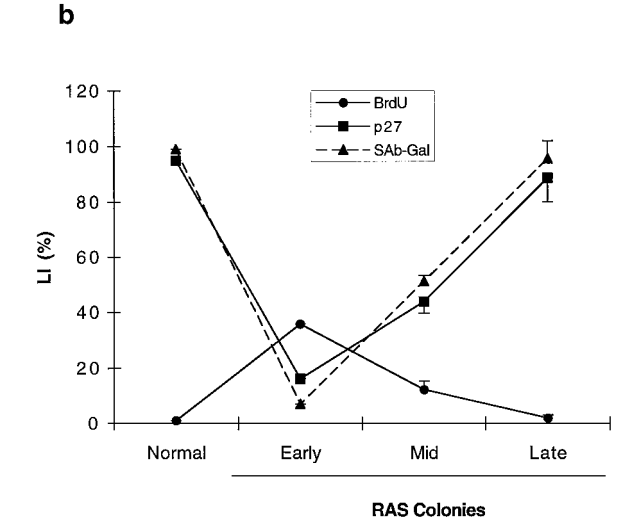

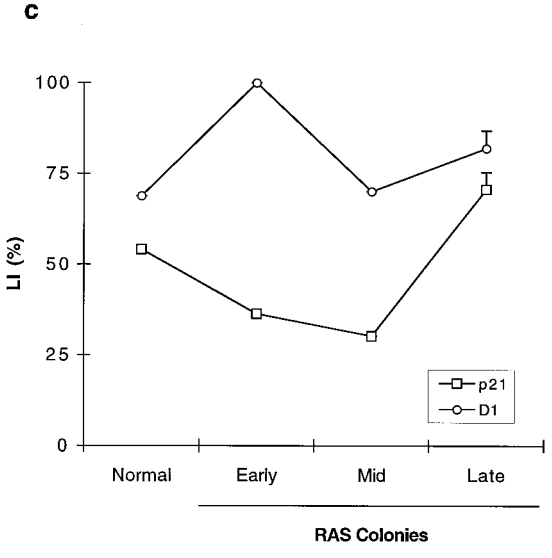

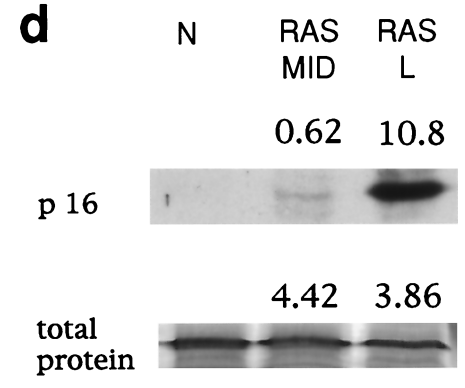

Increase in p16 signal in RAS-L vs RAS-MID corrected for total protein
= (10.8/3.86) x (4.42/0.62)
= 20-fold

FIG. 1—*Continued.*

T following infection with the retroviral vector psi-CRIP-SVU19 (6). Despite similar proliferation rates, and at similar sizes, colonies generated in this way failed to show any reduction in p27 expression (data not shown).

Spontaneous cessation of RAS-induced thyrocyte proliferation correlates with reexpression of nuclear p27 and de novo expression of $p16^{ink4a}$. RAS-induced growth ceased by 5 weeks postinfection at a final colony size varying from 10^4 to 10^6 cells. Colonies were analyzed as above at this and at intermediate time points postinfection. Growth arrest was associated with, and explicable by, a decline in BrdU LI, which eventually returned to normal levels (~1%), together with a corresponding restoration of SAβ-Gal expression and a flattened, senescence-like morphology (Fig. 1a).

The changes in p21 and cyclin D1 expression seen in early RAS colonies reverted to near-normal in terminally arrested colonies; however, the time course showed an imperfect correlation with BrdU LI at intermediate time points (Fig. 1c). In contrast, p27 expression showed a tight inverse correlation throughout with BrdU LI and a direct correlation with SAβ-Gal (Fig. 1b).

Given its established role in senescence in other cell types, we also examined expression of the CDK inhibitor $p16^{ink4a}$. There was a clear increase from undetectable levels in normal colonies to readily detectable levels in end-stage RAS colonies (Fig. 1a); however, the rather diffuse, predominantly cytoplasmic, pattern of immunostaining obtained with antibody DCS-50 was difficult to quantify microscopically. In this case, therefore, sufficient cells were collected to perform a limited Western blot analysis (Fig. 1d) which confirmed the absence of signal in normal cells and a 20-fold increase between proliferating (early) and arrested (end-stage) RAS colonies.

The possibility that the above changes were due simply to decreased mutant RAS expression in late-stage colonies, for example through methylation of the retroviral promoter, was excluded by analysis at both protein (Fig. 2a to d) and mRNA (Fig. 2e) levels, which confirmed the persistent overexpression of the mutant compared to the endogenous wild-type sequence in both early- and late-stage colonies.

Cessation of RAS-induced thyrocyte proliferation is not dependent on telomere erosion. Mean telomere length, measured as TRF size after *Hin*fI/*Rsa*I digestion of genomic DNA, varied from 9 to 11 kbp in different isolates of human thyrocytes at the end of their normal proliferative life span (Fig. 3).

Analysis of DNA from pooled RAS-induced colonies in comparison to the normal cells from which they were derived showed only variable, low-magnitude TRF shortening. In end-stage colonies this varied in different experiments from ~1.4 kbp down to unresolvable differences (Fig. 3a and b). Furthermore, the final mean TRF value (typically ~10 kbp) was always much larger than that observed in normal human fibroblasts at the end of their replicative life span (~7 kb in our hands) (Fig. 3b).

To address the possibility that normal thyrocytes, unlike fibroblasts and most other primary cultures, might circumvent telomere erosion through physiological expression of telomerase, we assayed telomerase activity in lysates using the well-established in vitro TRAP assay (32). No activity could be detected in any normal sample, nor in nearly all lysates of pooled RAS colonies at both early and late stages (Fig. 3c). Only one sample (Thy.1 RAS-E [Fig. 3c]) out of more than 30 analyzed was found to be positive, and this only at extremely weak levels (<1% of the positive control 293 cell line).

Finally we asked whether stable induction of telomerase activity through forced expression of the catalytic sub-unit of telomerase, hTERT, would, as in fibroblasts and several other

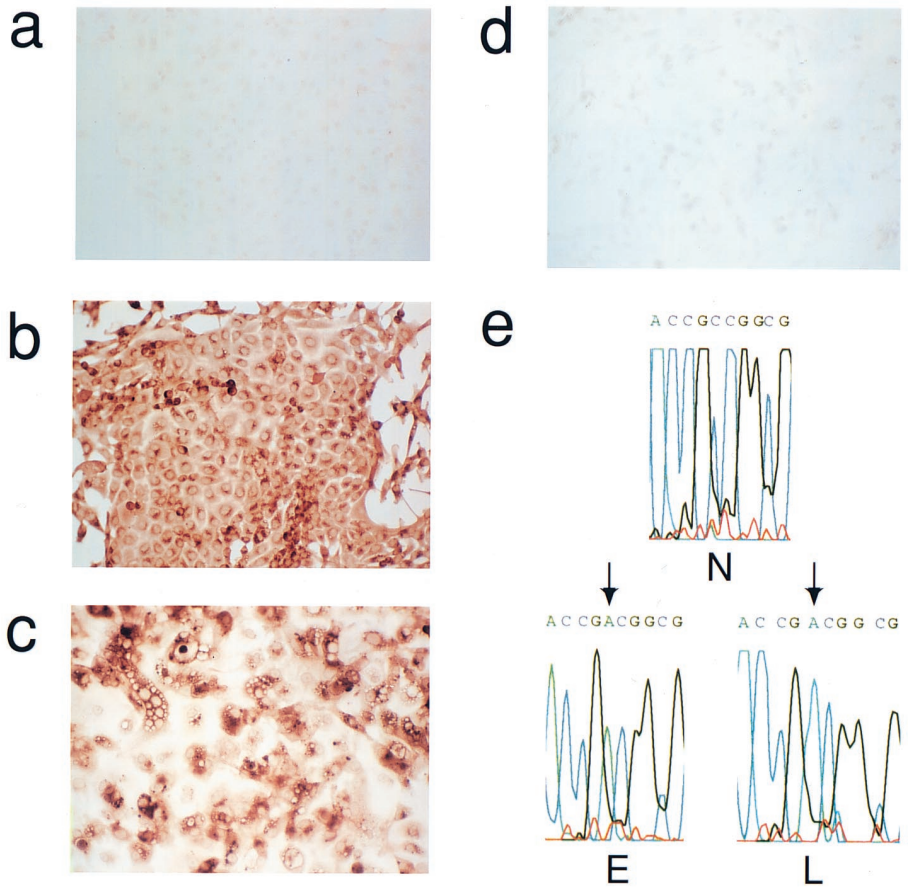

FIG. 2. Persistence of mutant RAS expression in late-stage RAS-induced colonies. (a to c) Immunocytochemical analysis of H-RAS protein using anti-ras antibody Y13-259 in normal thyroid cells (a); early, proliferating colonies induced by mutant H-RAS (b); and late-stage, growth-arrested colonies (c). (d) Late-stage colony immunostained with a species-matched antibody to an irrelevant antigen (polyomavirus large T) as negative control. Note that although antibody Y13-259 detects both mutant and wild-type RAS, comparison of panels b and c with normal (uninfected) thyroid cells (a) indicates that nearly all the immunostaining observed here can be attributed to the mutant protein (magnification, ×75). (e) Sequence (antisense) of cDNA surrounding codon 12 of H-RAS derived by RT-PCR of mRNA from normal (N), pooled early-stage (E), or late-stage (L) mutant RAS-induced colonies. The point mutation (arrowed) appears as a C→A transversion at position 2 of codon 12, equivalent to G→T in the coding sequence. Note that only mutant mRNA is detectable in both E and L, consistent with a much higher expression of the vector-encoded mutant RAS in both cases compared to the endogenous wild-type gene.

cell types (3), lead to an extension of replicative life span in RAS-induced colonies. Thyrocytes were infected with the V12H-RAS-neo vector as before, together with an in-house amphotropic vector (pBABEpuro-hTERT) (68) encoding hTERT together with puromycin resistance, or with the pBABEpuro vector without hTERT as a control. After selection in G418 plus puromycin, a similar yield of clones was obtained with or without hTERT expression.

Randomly selected groups of 20 colonies expressing mutant RAS alone and 20 expressing RAS and hTERT were followed up in detail. No differences in growth rate or morphology were seen (not shown), and both sets of colonies ceased proliferating after a similar time (4 to 5 weeks). Based on final colony cell counts (assuming no cell death), the mean numbers of PD undergone in the two groups were calculated as 13 (range, 9 to 15) and 12 (range, 9 to 14) respectively.

The phenotype of end-stage colonies expressing hTERT plus mutant RAS with respect to morphology, BrdU incorporation, SAβ-Gal staining, and expression of p21 and p27 was indistinguishable from that of the corresponding colonies generated by mutant RAS alone (compare Fig. 4 with Fig. 1).

The TRAP assay was performed on pooled RAS and hTERT colonies to check that the lack of effect on life span was not due to ineffective expression. A high level of activity was observed (Fig. 3c), comparable to that obtained in fibroblasts whose life span was successfully extended by infection with our hTERT vector (68).

Infection of normal thyrocytes with the pBABEpuro-hTERT vector alone failed to generate any colonies, either with or without puromycin selection.

These data indicate that terminal growth arrest occurring both in normal thyrocytes and in those expressing mutant RAS is regulated by a mechanism which comes into operation at mean telomere lengths well above those associated with senescence in fibroblasts and furthermore, unlike the latter, is not abrogated by forced expression of telomerase.

Expression of human papillomavirus (HPV) E7 fails to extend proliferative life span of thyrocyte colonies induced by mutant RAS. The correlation between spontaneous growth arrest in end-stage RAS-induced colonies and the increased expression of CDKIs p16 and p21 suggests that further tumor progression would require abrogation of one or both of these inhibitory controls. This is consistent with analyses of clinical samples (17) which have shown reduced expression of p27 in carcinomas compared to adenomas (although without evidence for mutation). Inactivating genomic abnormalities have

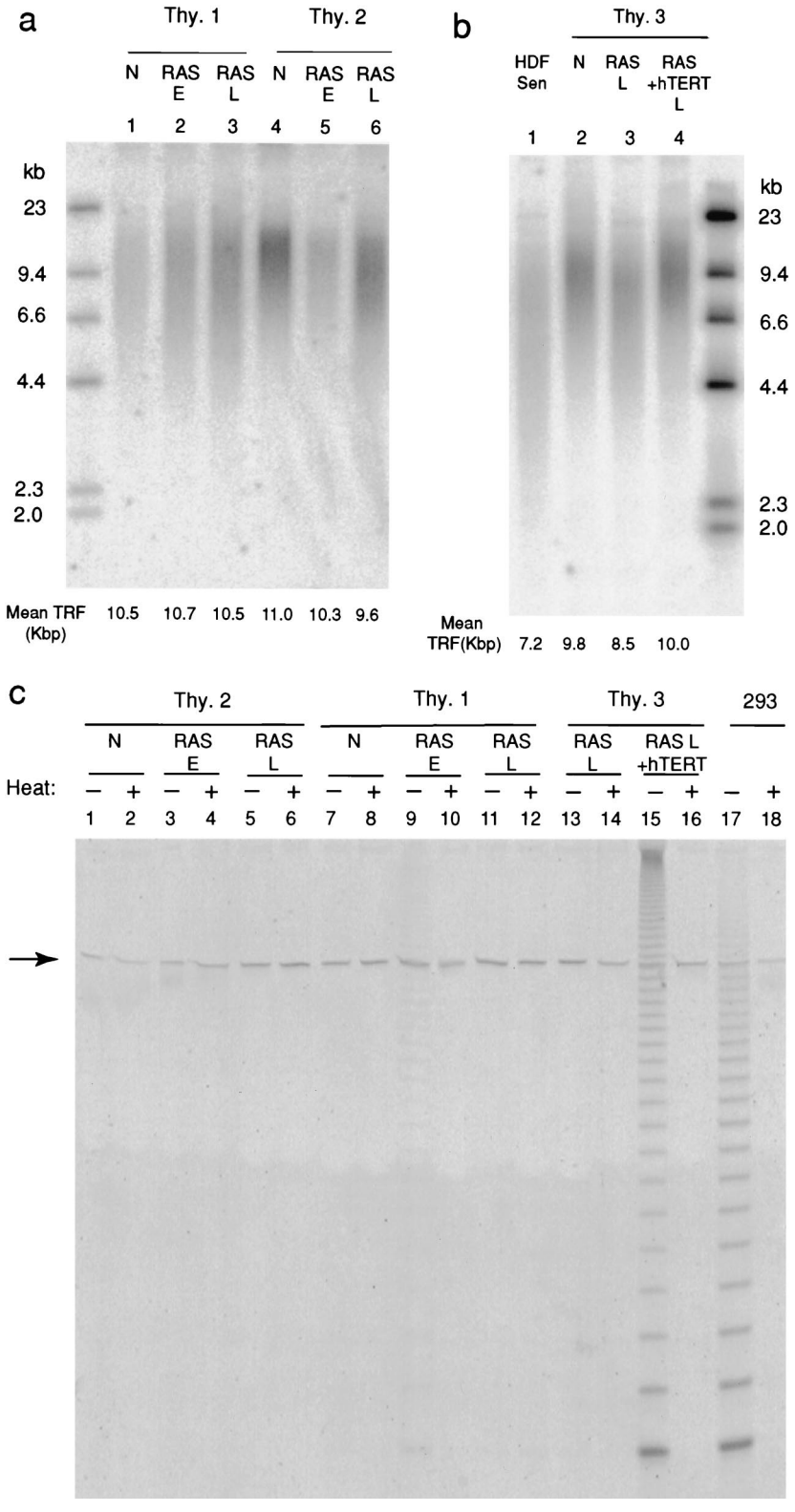

FIG. 3. Analysis of telomere length and telomerase activity in thyroid cells expressing mutant RAS. (a) TRF analysis of *Hin*fI/*Rsa*I-digested genomic DNA from normal thyrocytes (N), and pools of early (proliferating) (RAS E) and late-stage (RAS L) RAS colonies derived from two separate human thyroid samples (Thy.1 and Thy.2). Mean TRF values were calculated from densitometry data as described in text. (b) TRF analysis of normal (N) and late-stage (RAS L) RAS colonies derived from a third thyroid sample (Thy.3), together with colonies expressing both mutant RAS and the catalytic subunit of human telomerase (RAS + hTERT). Senescent human fibroblasts (strain HCA2) are shown for comparison (HDF SEN). (c) Telomerase activity assessed by TRAP assay in normal cells (N), in pools of early colonies expressing mutant RAS (RAS E) and late-stage colonies expressing mutant RAS alone (RAS L) or with hTERT (RAS L + hTERT). Each sample is analyzed with (+) or without (−) prior heat treatment (85°C for 10 min). The immortal human epithelial cell line 293 is included as a positive control. The arrow indicates the position of the internal telomerase amplification standard as a control for nonspecific PCR inhibition.

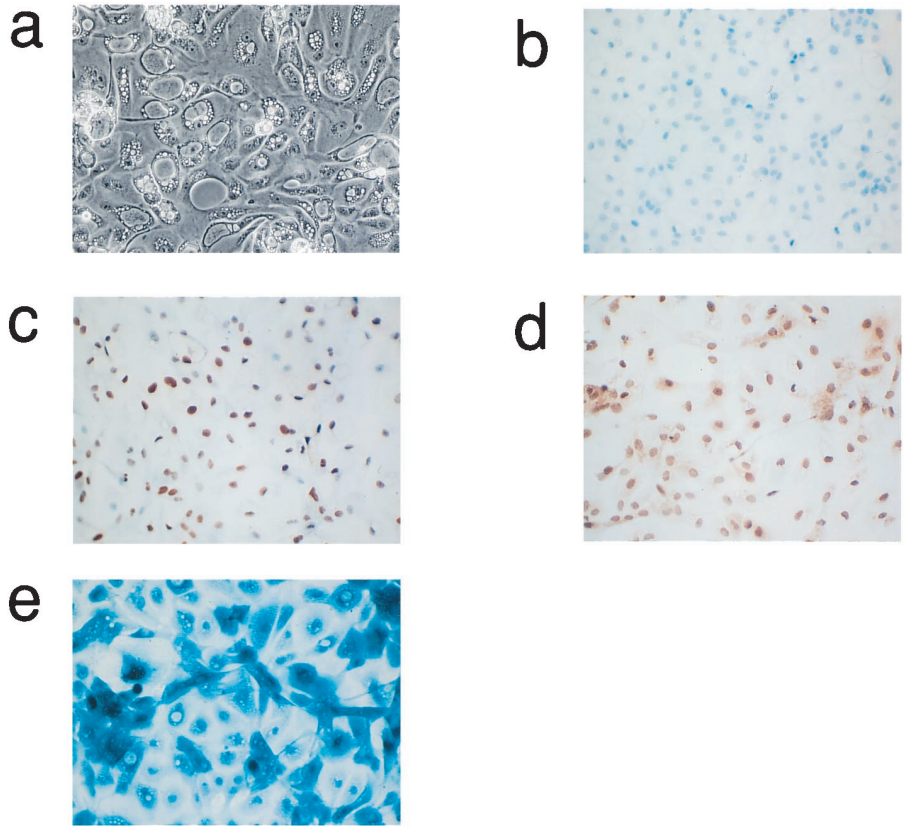

FIG. 4. Phenotype of end-stage thyroid epithelial colonies induced by coexpression of mutant RAS plus the catalytic subunit of telomerase, hTERT. Representative photomicrographs showing phase-contrast morphology (a), BrdU incorporation (all nuclei negative in this field) (b) and expression of $p21^{waf1}$ (c), $p27^{kip1}$ (d), and SAβ-Gal (e) as assessed as in Fig. 1. (b to d) These panels are lightly counterstained with hematoxilin. Magnification, ×50.

also been reported at the p16 locus, and we have observed promoter methylation or gene deletion in the majority of thyroid cancer cell lines and in up to 25% of well-differentiated thyroid cancers (27, 29, 70).

We therefore predicted that experimental abrogation of p16 and/or p27 function in thyrocytes expressing mutant RAS should confer a further extension of proliferative life span. Attempts to achieve this directly by anti-sense p27 or p16 expression have so far proven problematic; we therefore employed HPV E7 which is known to directly antagonise members of the p27 family of CDKIs and to block their effect downstream by inactivating Rb.

Thyrocytes were coinfected with the V12H RAS-neo vector together with either our pBABEpuro vector encoding E7, or pBABEpuro alone. Contrary to prediction, no significant difference in the final size of colonies was observed as a result of E7 expression, which was confirmed by immunocytochemical analysis (not shown). There was, however, a marked difference in the final fate of the E7-expressing colonies in that instead of reaching a viable quiescent end point they continued to proliferate, but with increasing cell death (Fig. 5) which finally resulted in colony degeneration. A terminal deoxynucleotidyltransferase-mediated dUTP-biotin nick end labeling (TUNEL) assay (not shown) confirmed that end-stage E7/RAS colonies were undergoing apoptosis. A similar outcome was seen if the E7 vector was replaced with one encoding both E7

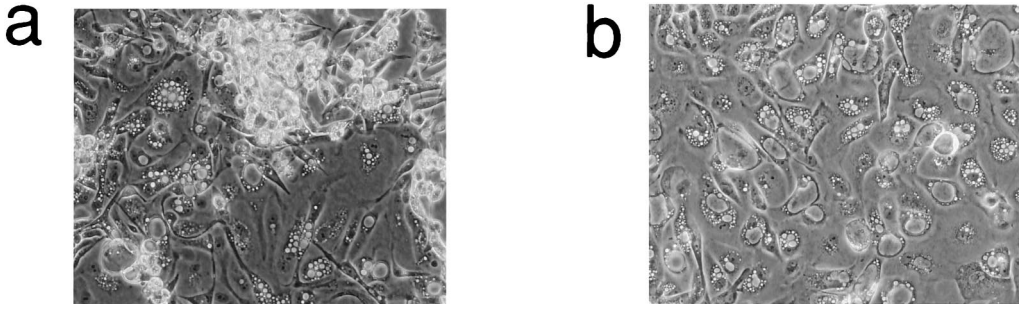

FIG. 5. Coexpression of HPV E7 plus mutant RAS changes the end-stage phenotype of thyroid epithelial clones to cell death rather than growth arrest. Phase-contrast photomicrographs of typical late-stage colonies generated either by mutant RAS plus HPV E7 (a) or mutant RAS alone (b). Note the much more marked cell death and detachment in panel a. Magnification, ×50.

and E6, indicating that, as observed previously (4), apoptosis in thyrocytes is p53 independent.

DISCUSSION

Mechanisms underlying the sensitivity of thyroid epithelial cells to RAS-induced proliferation. The prolonged growth stimulation induced by activated RAS in normal thyroid epithelial cells stands in sharp contrast to the response observed in normal human fibroblasts, in which proliferation is limited within a few PD by the onset of a permanent growth arrest state, which, apart from being independent of telomere erosion (65), closely resembles replicative senescence mediated by both $p14^{arf}$-p53 and $p16^{ink4a}$ pathways (39, 55, 73).

This premature senescence phenotype, which we too have observed in fibroblasts, has aroused great interest recently (51) as a potential innate tumor suppressor mechanism and an explanation for the selective pressure for mutation of p53 and/or p16 in tumors bearing *RAS* mutations (39, 73).

This concept does not fit well, however, with observations on epithelial tumor models both in vivo (18, 36, 58) and in vitro (4, 37; this study), which indicate the ability of *RAS* mutation to drive sustained proliferation for at least 20 PD without apparent mutation of these tumor suppressor pathways. Furthermore, it is implausible, even on purely probabilistic grounds, that the few PD available before onset of permanent RAS-induced senescence would afford any reasonable chance of a cell acquiring the necessary tumor suppressor gene mutation(s) for further clonal expansion.

We suggest rather that premature senescence effectively renders tumor induction by RAS impossible in those cell types, such as fibroblasts, in which it occurs and hence accounts for the observed lack of involvement of this oncogene family in those (rare) tumors derived from them, e.g., fibrosarcomas (9). Conversely, it is the absence of this mechanism which confers on cells such as thyrocytes their susceptibility to RAS-induced tumorigenesis. The pattern of expression of CDKIs reported here provides an initial insight into the underlying differences in cell-cycle regulatory pathways which may explain this crucial context-dependent difference in response to RAS activation.

In fibroblasts (55, 73), RAS-induced senescence is associated with large increases in cellular content of two CDKIs—p16 and p21—the latter being driven by activation of p53, in turn, probably resulting from increased levels of $p14^{arf}$ (51). In thyrocytes, in contrast, there is no early RAS-induced increase in p21 or p16; on the contrary there is a dramatic fall in the level of another p21 family member, $p27^{KIP1}$, which does not occur in fibroblasts (73). The predicted effect of this is a release of inhibition of CDKs controlling G_1/S transition, either directly or, as suggested recently (12, 45, 57), via a redistribution of p21 from CDK2-cyclin E to CDK4-cyclin D complexes, hence increasing CDK2 activity. It is likely therefore that the net level of CDKI activity is altered in opposite directions in thyrocytes and fibroblasts following RAS activation.

p27 is expressed at high levels in normal thyrocytes both in vitro (this study) and in the intact thyroid gland, in both human (17, 40, 60) and mouse (13). Many studies suggest that p27 plays a role in growth arrest accompanying differentiation (16, 49, 72), and p27-null mice exhibit hyperplasia of many highly differentiated cell populations, including endocrine glands (19, 33, 47) (although thyroid was not specifically studied). Taken together, this suggests that p27 is necessary for maintaining the normally very low proliferative rate of thyrocytes in vivo and that its loss is a plausible candidate mechanism for induction of inappropriate proliferation in these cells.

RAS activation has been shown to induce destabilization of p27 in many different experimental models, in most cases probably through ubiquitin-mediated degradation (31, 38, 50, 59). Although other pathways such as RAF-mitogen-activated protein kinase may be necessary in some contexts (31), the consensus currently favors rho as a key effector for this response (25, 64). rho is also an attractive candidate in our model, since its degree of activation has been previously reported in a fibroblast model (48) to determine whether or not RAS induces p21 and hence premature senescence. We speculate therefore that in thyrocytes and other epithelial cells susceptible to RAS-induced tumorigenesis, in contrast to refractory cell types such as fibroblasts, the level of activation of rho in response to RAS signalling is sufficient, firstly, to prevent induction of p21 by other RAS effector pathway(s) and, secondly, to induce destabilization of p27. In related work (22), we recently established the requirement for at least two effector pathways in RAS-induced thyrocyte proliferation—mitogen-activated protein kinase and phosphatidyl inositol 3-kinase. The former is a good candidate for the induction of cyclin D1 by mutant RAS (25, 41), while the latter may be responsible at least in part for activation of rho (although we have not yet excluded a role for the Ral-GDS effector pathway).

How rho destabilizes p27 is still unclear. While some studies point to a direct action (38), others (25) suggest that it is secondary to activation of CDK2-cyclin E (by other means), leading to increased CDK2-mediated phosphorylation of p27, which is known to be a key modification targeting it for ubiquitin-mediated degradation (56, 61, 62). In other words, p27 degradation may be both upstream and downstream of CDK2 activation, thus creating a positive feedback loop which greatly complicates attempts to establish cause-effect relationships.

Clearly, further work will be needed to establish the precise role of p27 degradation in RAS-induced proliferation in our model. Nevertheless, the data presented here already open up a route to identifying the molecular determinants of susceptibility to RAS-induced tumorigenesis, which in turn may provide novel therapeutic targets.

Mechanisms limiting RAS-induced clonal expression: an antioncogenic PLB not mediated by a telomere clock. Proliferation of thyroid epithelial cells induced by mutant *RAS* ceases spontaneously after 15 to 25 PD despite continued expression of the activated oncogene. This growth arrest is correlated with, and potentially mediated by, increases in two CDKIs, p27 and p16. Although these may act redundantly, recent insights into cell cycle control (12, 57) suggest a simpler, sequential model driven solely by induction of p16 expression after a given number of PD. In addition to its direct inhibitory action on CDK4 and CDK6, it is now known that an increase in p16 can also lead to displacement of p21 from CDK4 or CDK6 to CDK2-cyclin E complexes, resulting indirectly in reduced activity of the latter, an effect which may be further enhanced by formation of inactive complexes between CDK2 and displaced cyclin D1 (44). Loss of CDK2 activity will reduce the phosphorylation of p27 and hence lead to an increase in its steady-state level, an effect which should be amplified by the feedback loop (56) which results from further inhibition of CDK2. On this model, therefore, the stabilization of p27, though triggered in the first instance by the increase in p16, may nevertheless be necessary to ensure sufficient inhibition of CDKs for complete growth arrest.

The above model is consistent with analyses of human thyroid cancers (17, 42, 60, 63) and derived cell lines (27, 29), which frequently show loss of p16 and/or decreased p27 expression in cancers compared to normal or benign epithelia, suggesting that loss of either CDKI may permit escape from the PLB limiting initial clonal expansion driven by RAS. Un-

fortunately, we have not as yet been able to test this prediction experimentally by direct manipulation of p27 or p16. A more central abrogation of this TSG pathway using HPV E7 was of limited value, since although appearing to relieve proliferative arrest, net growth was offset by increasing cell death.

A key finding in the current work is the apparent independence of the above-mentioned PLB on telomere erosion, as shown most conclusively by the failure of experimentally induced telomerase activity to extend life span despite stabilization of telomere length. We must, therefore, postulate the existence of a separate cell division counting mechanism, which acts at least in part via induction of p16. Such a clock also seems to operate in controlling physiological (growth factor induced) proliferative life span in a variety of situations, including primary fibroblasts in rodents (54) and, moreover, several specific types of human epithelium, including mammary epithelial cells (20, 34), keratinocytes (34) and uroepithelial cells (53, 71) which undergo senescence after a similar range of PD (10 to 30 PD). The originality of our observation is that it demonstrates a crucial role for a p16-dependent, telomere-independent PLB in limiting not only physiological but also oncogene-driven proliferation.

In all of these situations the major question which remains is the link between replicative age (elapsed divisions) and induction of p16 expression. Demethylation of promoter sequences clearly plays a part in this (20, 26) and there is long-standing evidence for reduction in DNA methylation during replicative ageing (24); the mechanistic details of such a clock, however, and the role of potential *trans*-acting factors such as BMI-1 (28) remain obscure. Given its potential importance as a natural tumor suppressor mechanism alternative to telomere erosion, this promises to be an area of major basic and therapeutic significance.

ACKNOWLEDGMENTS

We thank the Cancer Research Campaign and the Medical Research Council for grant support.

We also thank Michèle Haughton for primary cells and Theresa King for manuscript and graphics preparation.

REFERENCES

1. **Almoguera, C., D. Shibata, K. Forrester, J. Martin, N. Arnheim, and M. Perucho.** 1988. Most human carcinomas of the exocrine pancreas contain mutant c-K-ras genes. Cell **53:**549–554.
2. **Bartkova, J., J. Lukas, M. Strauss, and J. Bartek.** 1998. Cyclin D3: requirement for G1/S transition and high abundance in quiescent tissues suggest a dual role in proliferation and differentiation. Oncogene **17:**1027–1037.
3. **Bodnar, A. G., M. Ouellette, M. Frolkis, S. E. Holt, C.-P. Chiu, G. B. Morin, C. B. Harley, J. W. Shay, S. Lichtsteiner, and W. E. Wright.** 1998. Extension of life-span by introduction of telomerase into normal human cells. Science **279:**349–352.
4. **Bond, J., M. Haughton, J. Rowson, V. Gire, D. Wynford-Thomas, and F. Wyllie.** 1999. Control of replicative life span in human cells: barriers to clonal expansion intermediate between M1 senescence and M2 crisis. Mol. Cell. Biol. **19:**3103–3114.
5. **Bond, J. A., F. S. Wyllie, and D. Wynford-Thomas.** 1994. Escape from senescence in human diploid fibroblasts induced directly by mutant p53. Oncogene **9:**1885–1889.
6. **Bond, J. A., G. O. Ness, J. Rowson, M. Ivan, D. White, and D. Wynford-Thomas.** 1996. Spontaneous de-differentiation correlates with extended lifespan in transformed thyroid epithelial cells: an epigenetic mechanism of tumour progression. Int. J. Cancer **67:**563–572.
7. **Bond, J. A., F. S. Wyllie, J. Rowson, A. Radulescu, and D. Wynford-Thomas.** 1994. In vitro reconstruction of tumour initiation in a human epithelium. Oncogene **9:**281–290.
8. **Bos, J. L., E. R. Fearon, S. R. Hamilton, M. Verlaan-de Vries, J. H. van Boom, A. J. van der Eb, and B. Vogelstein.** 1987. Prevalence of ras gene mutations in human colorectal cancers. Nature **327:**293–297.
9. **Bos, J. L.** 1989. Ras oncogenes in human cancer: a review. Cancer Res. **49:**4682–4689.
10. **Broccoli, D., J. W. Young, and T. de Lange.** 1995. Telomerase activity in normal and malignant hematopoietic cells. Proc. Natl. Acad. Sci. USA **92:**9082–9086.
11. **Brown, J. P., W. Wenyi, and J. M. Sedivy.** 1997. Bypass of senescence after disruption of p21CIP1/WAF1 gene in normal diploid human fibroblasts. Science **277:**831–834.
12. **Cheng, M., P. Olivier, J. A. Diehl, M. Fero, M. F. Roussel, J. M. Roberts, and C. J. Sherr.** 1999. The p21(Cip1) and p27(Kip1) CDK 'inhibitors' are essential activators of cyclin D-dependent kinases in murine fibroblasts. EMBO J. **18:**1571–1583.
13. **Coppee, F., F. Depoortere, J. Bartek, C. Ledent, M. Parmentier, and J. E. Dumont.** 1998. Differential patterns of cell cycle regulatory proteins expression in transgenic models of thyroid tumours. Oncogene **17:**631–641.
14. **Depoortere, F., A. Van Keymeulen, J. Lukas, S. Costagliola, J. Bartkova, J. E. Dumont, J. Bartek, P. P. Roger, and S. Dremier.** 1998. A requirement for cyclin D3-cyclin-dependent kinase (cdk)-4 assembly in the cyclic adenosine monophosphate-dependent proliferation of thyrocytes. J. Cell Biol. **140:**1427–1439.
15. **Dimri, G. P., X. Lee, G. Basile, M. Acosta, G. Scott, C. Roskelley, E. E. Medrano, M. Linskens, I. Rubelj, O. Pereira-Smith, M. Peacocke, and J. Campisi.** 1995. A biomarker that identifies senescent human cells in culture and in aging skin in vivo. Proc. Natl. Acad. Sci. USA **92:**9363–9367.
16. **Durand, B., M. L. Fero, J. M. Roberts, and M. C. Raff.** 1998. p27Kip1 alters the response of cells to mitogen and is part of a cell-intrinsic timer that arrests the cell cycle and initiates differentiation. Curr. Biol. **8:**431–440.
17. **Erickson, L. A., L. Jin, P. C. Wollan, G. B. Thompson, J. van Heerden, and R. V. Lloyd.** 1998. Expression of p27kip1 and Ki-67 in benign and malignant thyroid tumors. Mod. Pathol. **11:**169–174.
18. **Fearon, E. R., and B. Vogelstein.** 1990. A genetic model for colorectal tumorigenesis. Cell **61:**759–767.
19. **Fero, M. L., M. Rivkin, M. Tasch, P. Porter, C. E. Carow, E. Firpo, K. Polyak, L. H. Tsai, V. Broudy, R. M. Perlmutter, K. Kaushansky, and J. M. Roberts.** 1996. A syndrome of multiorgan hyperplasia with features of gigantism, tumorigenesis, and female sterility in p27(Kip1)-deficient mice. Cell **85:**733–744.
20. **Foster, S. A., D. J. Wong, M. T. Barrett, and D. A. Galloway.** 1998. Inactivation of p16 in human mammary epithelial cells by CpG island methylation. Mol. Cell. Biol. **18:**1793–1801.
21. **Gire, V., and D. Wynford-Thomas.** 1998. Reinitiation of DNA synthesis and cell division in senescent human fibroblasts by microinjection of anti-p53 antibodies. Mol. Cell. Biol. **18:**1611–1621.
22. **Gire, V., C. J. Marshall, and D. Wynford-Thomas.** 1999. Activation of mitogen-activated protein kinase is necessary but not sufficient for proliferation of human thyroid epithelial cells induced by mutant Ras. Oncogene **18:**4819–4832.
23. **Hirai, A., S. Nakamura, Y. Noguchi, T. Yasuda, M. Kitagawa, I. Tatsuno, T. Oeda, K. Tahara, T. Terano, S. Narumiya, L. D. Kohn, and Y. Saito.** 1997. Geranylgeranylated rho small GTPase(s) are essential for the degradation of p27Kip1 and facilitate the progression from G1 to S phase in growth-stimulated rat FRTL-5 cells. J. Biol. Chem. **272:**13–16.
24. **Holliday, R.** 1996. Endless quest. Bioessays **18:**3–5.
25. **Hu, W., C. J. Bellone, and J. J. Baldassare.** 1999. RhoA stimulates p27(Kip) degradation through its regulation of cyclin E/CDK2 activity. J. Biol. Chem. **274:**3396–3401.
26. **Huschtscha, L. I., J. R. Noble, A. A. Neumann, E. L. Moy, P. Barry, J. R. Melki, S. J. Clark, and R. R. Reddel.** 1998. Loss of p16INK4 expression by methylation is associated with lifespan extension of human mammary epithelial cells. Cancer Res. **58:**3508–3512.
27. **Ivan, M., D. Wynford-Thomas, and C. J. Jones.** 1996. Abnormalities of the p16INK4a gene in thyroid cancer cell lines. Eur. J. Cancer **32:**2369–2370.
28. **Jacobs, J., K. Kieboom, S. Marino, R. de Pinho, and M. van Lohuizen.** 1999. The oncogene and polycomb-group gene bmi-1 regulates cell proliferation and senescence through the ink4a locus. Nature **397:**164–168.
29. **Jones, C. J., J. J. Shaw, F. S. Wyllie, N. Gaillard, M. Schlumberger, and D. Wynford-Thomas.** 1996. High frequency deletion of the tumour suppressor gene P16INK4a (MTS1) in human thyroid cancer cell lines. Mol. Cell. Endocrinol. **116:**115–119.
30. **Jones, C. J., A. Soley, J. W. Skinner, J. Gupta, M. F. Haughton, F. S. Wyllie, M. Schlumberger, S. Bacchetti, and D. Wynford-Thomas.** 1998. Dissociation of telomere dynamics from telomerase activity in human thyroid cancer cells. Exp. Cell Res. **240:**333–339.
31. **Kawada, M., S. Yamagoe, Y. Murakami, K. Suzuki, S. Mizuno, and Y. Uehara.** 1997. Induction of p27Kip1 degradation and anchorage independence by Ras through the MAP kinase signaling pathway. Oncogene **15:**629–637.
32. **Kim, N. W., M. A. Piatyszek, K. R. Prowse, C. B. Harley, M. D. West, P. L. C. Ho, G. M. Coviello, W. E. Wright, S. L. Weinrich, and J. W. Shay.** 1994. Specific association of human telomerase activity with immortal cells and cancer. Science **266:**2011–2015.
33. **Kiyokawa, H., R. D. Kineman, K. O. Manova-Todorova, V. C. Soares, E. S. Hoffman, M. Ono, D. Khanam, A. C. Hayday, L. A. Frohman, and A. Koff.** 1996. Enhanced growth of mice lacking the cyclin-dependent kinase inhibitor function of p27(Kip1). Cell **85:**721–732.
34. **Kiyono, T., S. A. Foster, J. I. Koop, J. K. McDougall, D. A. Galloway, and A. J. Klingelhutz.** 1998. Both Rb/p16INK4a inactivation and telomerase

activity are required to immortalize human epithelial cells. Nature **396:**84–88.
35. **Kruk, P. A., N. J. Rampino, and V. A. Bohr.** 1995. DNA damage and repair in telomeres: relation to aging. Proc. Natl. Acad. Sci. USA **92:**258–262.
36. **Lemoine, N. R., E. S. Mayall, F. S. Wyllie, E. D. Williams, M. Goyns, B. Stringer, and D. Wynford-Thomas.** 1989. High frequency of ras oncogene activation in all stages of human thyroid tumorigenesis. Oncogene **4:**159–164.
37. **Lemoine, N. R., S. Staddon, J. Bond, F. S. Wyllie, J. J. Shaw, and D. Wynford-Thomas.** 1990. Partial transformation of human thyroid epithelial cells by mutant Ha-ras oncogene. Oncogene **5:**1833–1837.
38. **Leone, G., J. DeGregori, R. Sears, L. Jakoi, and J. R. Nevins.** 1997. Myc and Ras collaborate in inducing accumulation of active cyclin E/Cdk2 and E2F. Nature **387:**422–426.
39. **Lin, A. W., M. Barradas, J. C. Stone, L. van Aelst, M. Serrano, and S. W. Lowe.** 1998. Premature senescence involving p53 and p16 is activated in response to constitutive MEK/MAPK mitogenic signaling. Genes Dev. **12:**3008–3019.
40. **Lloyd, A. C.** 1998. Ras versus cyclin-dependent kinase inhibitors. Curr. Opin. Genet. Dev **8:**43–48.
41. **Lloyd, R. V., L. Jin, X. Qian, and E. Kulig.** 1997. Aberrant p27kip1 expression in endocrine and other tumors. Am. J. Pathol. **150:**401–407.
42. **Lloyd, R. V., L. A. Erickson, L. Jin, E. Kulig, X. Qian, J. C. Cheville, and B. W. Scheithauer.** 1999. p27kip1: a multifunctional cyclin-dependent kinase inhibitor with prognostic significance in human cancers. Am. J. Pathol. **154:**313–323.
43. **Lukas, J., D. Parry, L. Aagaard, D. J. Mann, J. Bartkova, M. Strauss, G. Peters, and J. Bartek.** 1995. Retinoblastoma-protein-dependent cell-cycle inhibition by the tumour suppressor p16. Nature **375:**503–506.
44. **Lukas, J., C. S. Sorensen, C. Lukas, E. Santoni-Rugiu, and J. Bartek.** 1999. p16INK4a, but not constitutively active pRb, can impose a sustained G1 arrest: molecular mechanisms and implications for oncogenesis. Oncogene **18:**3930–3935.
45. **Mitra, J., C. Y. Dai, K. Somasundaram, W. S. El-Deiry, K. Satyamoorthy, M. Herlyn, and G. H. Enders.** 1999. Induction of $p21^{WAF1/CIP1}$ and inhibition of Cdk2 mediated by the tumor suppressor $p16^{INK4a}$. Mol. Cell. Biol. **19:**3916–3928.
46. **Morgenstern, J. P., and H. Land.** 1990. Advanced mammalian gene transfer: high titre retroviral vectors with multiple drug selection markers and a complementary helper-free packaging cell line. Nucleic Acids Res. **18:**3587–3596.
47. **Nakayama, K., N. Ishida, M. Shirane, A. Inomata, T. Inoue, N. Shishido, I. Horii, and D. Y. Loh.** 1996. Mice lacking p27(Kip1) display increased body size, multiple organ hyperplasia, retinal dysplasia, and pituitary tumors. Cell **85:**707–720.
48. **Olson, M. F., H. F. Paterson, and C. J. Marshall.** 1998. Signals from Ras and Rho GTPases interact to regulate expression of p21Waf1/Cip1. Nature **394:**295–299.
49. **Onishi, T., and K. Hruska.** 1997. Expression of p27Kip1 in osteoblast-like cells during differentiation with parathyroid hormone. Endocrinology **138:**1995–2004.
50. **Pagano, M., S. W. Tam, A. M. Theodoras, P. Beer-Romero, G. Del Sal, V. Chau, P. R. Yew, G. F. Draetta, and M. Rolfe.** 1995. Role of the ubiquitin-proteasome pathway in regulating abundance of the cyclin-dependent kinase inhibitor p27. Science **269:**682–685.
51. **Palmero, I., C. Pantoja, and M. Serrano.** 1998. p19ARF links the tumour suppressor p53 to Ras. Nature **395:**125–126.
52. **Reddel, R.** 1998. A reassessment of the telomere hypothesis of senescence. Bioessays **20:**977–984.
53. **Reznikoff, C. A., T. R. Yeager, C. D. Belair, E. Savelieva, J. A. Puthenveettil, and W. M. Stadler.** 1996. Elevated p16 at senescence and loss of 16 at immortalization in human papillomavirus 16 E6, but not E7, transformed human uroepithelial cells. Cancer Res. **56:**2886–2890.
54. **Russo, I., A. R. Silver, A. P. Cuthbert, D. K. Griffin, D. A. Trott, and R. F. Newbold.** 1998. A telomere-independent senescence mechanism is the sole barrier to Syrian hamster cell immortalization. Oncogene **17:**3417–3426.
55. **Serrano, M., A. W. Lin, M. E. McCurrach, D. Beach, and S. W. Lowe.** 1997. Oncogenic ras provokes premature cell senescence associated with accumulation of p53 and p16INK4a. Cell **88:**593–602.
56. **Sheaff, R. J., M. Groudine, M. Gordon, J. M. Roberts, and B. E. Clurman.** 1997. Cyclin E-CDK2 is a regulator of p27Kip1. Genes Dev. **11:**1464–1478.
57. **Sherr, C. J., and J. M. Roberts.** 1999. CDK inhibitors: positive and negative regulators of G1-phase progression. Genes Dev. **13:**1501–1512.
58. **Suarez, H. G., J. A. du Villard, M. Severino, B. Caillou, M. Schlumberger, M. Tubiana, C. Parmentier, and R. Monier.** 1990. Presence of mutations of all three ras genes in human thyroid tumours. Oncogene **5:**565–570.
59. **Takuwa, N., and Y. Takuwa.** 1997. Ras activity late in G_1 phase required for $p27^{kip1}$ downregulation, passage through the restriction point, and entry into S phase in growth factor-stimulated NIH 3T3 fibroblasts. Mol. Cell. Biol. **17:**5348–5358.
60. **Tallini, G., G. Garcia-Rostan, A. Herrero, D. Zelterman, G. Viale, S. Bosari, and M. L. Carcangiu.** 1999. Downregulation of p27KIP1 and Ki67/Mib1 labeling index support the classification of thyroid carcinoma into prognostically relevant categories. Am. J. Surg. Pathol. **23:**678–685.
61. **Tsvetkov, L. M., K. H. Yeh, S. J. Lee, H. Sun, and H. Zhang.** 1999. p27(Kip1) ubiquitination and degradation is regulated by the SCF(Skp2) complex through phosphorylated Thr187 in p27. Curr. Biol. **9:**661–664.
62. **Vlach, J., S. Hennecke, and B. Amati.** 1997. Phosphorylation-dependent degradation of the cyclin-dependent kinase inhibitor p27. EMBO J. **16:**5334–5344.
63. **Wang, S., J. Wuu, L. Savas, N. Patwardhan, and A. Khan.** 1998. The role of cell cycle regulatory proteins, cyclin D1, cyclin E, and p27 in thyroid carcinogenesis. Hum. Pathol. **29:**1304–1309.
64. **Weber, J. D., W. Hu, S. C. Jefcoat, Jr., D. M. Raben, J. J. Baldassare.** 1997. Ras-stimulated extracellular signal-related kinase 1 and RhoA activities coordinate platelet-derived growth factor-induced G1 progression through the independent regulation of cyclin D1 and p27. J. Biol. Chem. **272:**32966–32971.
65. **Wei, S., and J. M. Sedivy.** 1999. Expression of catalytically active telomerase does not prevent premature senescence caused by overexpression of oncogenic Ha-Ras in normal human fibroblasts. Cancer Res. **59:**1539–1543.
66. **Williams, D. W., E. D. Williams, and D. Wynford-Thomas.** 1988. Loss of dependence in IGF-1 for proliferation of human thyroid adenoma cells. Br. J. Cancer **57:**535–539.
67. **Wright, W. E., J. W. Shay, and M. A. Piatyszek.** 1995. Modifications of a telomeric repeat amplification protocol (TRAP) result in increased reliability, linearity and sensitivity. Nucleic Acids Res. **23:**3794–3795.
68. **Wyllie, F. S., C. J. Jones, J. W. Skinner, M. F. Haughton, C. Wallis, D. Wynford-Thomas, R. G. Faragher, and D. Kipling.** 2000. Telomerase prevents the accelerated cell ageing of Werner syndrome fibroblasts. Nat. Genet. **24:**16–17.
69. **Wynford-Thomas, D.** 1999. Cellular senescence and cancer. J. Pathol. **187:**100–111.
70. **Wynford-Thomas, D.** 1999. Molecular basis of tumour initiation and progression in the thyroid follicular cell: in vitro models, p. 225–238. *In* G. Thomas, A. Karaoglov, and E. D. Williams (ed.), Radiation and thyroid cancer. World Scientific, London, United Kingdom.
71. **Yeager, T. R., S. DeVries, D. F. Jarrard, C. Kao, S. Y. Nakada, T. D. Moon, R. Bruskewitz, W. M. Stadler, L. F. Meisner, K. W. Gilchrist, M. A. Newton, F. M. Waldman, and C. A. Reznikoff.** 1998. Overcoming cellular senescence in human cancer pathogenesis. Genes Dev. **12:**163–174.
72. **Zabludoff, S. D., M. Csete, R. Wagner, X. Yu, and B. J. Wold.** 1998. p27Kip1 is expressed transiently in developing myotomes and enhances myogenesis. Cell Growth Differ. **9:**1–11.
73. **Zhu, J., D. Woods, M. McMahon, and J. M. Bishop.** 1998. Senescence of human fibroblasts induced by oncogenic Raf. Genes Dev. **12:**2997–3007.